TU Delft

Delft University of Technology

Lipid bilayers cushioned with polyelectrolyte-based films on doped silicon surfaces

Poltorak, Lukasz; Verheijden, Mark L.; Bosma, Duco; Jonkheijm, Pascal; de Smet, Louis C.P.M.; Sudhölter, Ernst J.R.

DOI
10.1016/j.bbamem.2018.09.018

Publication date
2018

Document Version
Accepted author manuscript

Published in
Biochimica et Biophysica Acta - Biomembranes

Citation (APA)
Poltorak, L., Verheijden, M. L., Bosma, D., Jonkheijm, P., de Smet, L. C. P. M., & Sudhölter, E. J. R. (2018). Lipid bilayers cushioned with polyelectrolyte-based films on doped silicon surfaces. *Biochimica et Biophysica Acta - Biomembranes*, *1860*(12), 2669-2680. https://doi.org/10.1016/j.bbamem.2018.09.018

Important note
To cite this publication, please use the final published version (if applicable).
Please check the document version above.

Copyright
Other than for strictly personal use, it is not permitted to download, forward or distribute the text or part of it, without the consent of the author(s) and/or copyright holder(s), unless the work is under an open content license such as Creative Commons.

Takedown policy
Please contact us and provide details if you believe this document breaches copyrights.
We will remove access to the work immediately and investigate your claim.

This work is downloaded from Delft University of Technology.
For technical reasons the number of authors shown on this cover page is limited to a maximum of 10.

Lipid bilayers cushioned with polyelectrolyte-based films on doped silicon surfaces

Lukasz Poltorak,*[1] Mark L. Verheijden,[2] Duco Bosma, [1] Pascal Jonkheijm,[2] Louis C. P. M. de Smet,[1,3] Ernst J. R. Sudhölter[1]

1) Delft University of Technology, Department of Chemical Engineering, Van der Maasweg 9, 2629 HZ Delft, The Netherlands
2) Molecular Nanofabrication Group of the MESA+ Institute for Nanotechnology and Bioinspired Molecular Engineering Laboratory of the MIRA Institute for Biomedical Technology and Technical Medicine, Department of Science and Technology, University of Twente, P.O. Box 217, 7500 AE, Enschede, The Netherlands
3) Wageningen University & Research, Laboratory of Organic Chemistry, Stippeneng 4, 6708 WE Wageningen, The Netherlands

*Corresponding author: l.poltorak@tudelft.nl

Keywords: supported lipid bilayer; thin polymeric cushion; electrochemical impedance spectroscopy; silicon semiconductor; layer-by-layer deposition

Abstract

Silicon semiconductors with a thin surface layer of silica were first modified with polyelectrolytes (polyethyleneimine, polystyrene sulfonate and poly(allylamine)) via a facile layer-by-layer deposition approach. Subsequently, lipid vesicles were added to the preformed polymeric cushion, resulting in the adsorption of intact vesicles or fusion and lipid bilayer formation. To study involved interactions we employed optical reflectometry, electrochemical impedance spectroscopy and fluorescent recovery after photo bleaching. Three phospholipids with different charge of polar head groups, *i.e.* 1,2-dioleoyl-sn-glycero-3-phosphocholine (DOPC), 1,2-dioleoyl- sn-glycero-3-phospho-L-serine (DOPS) and 1,2-dioleoyl-3-trimethylammonium-propane (DOTAP) were used to prepare vesicles with varying surface charge. We observed that only lipid vesicles composed from 1:1 (mole:mole) mixture of DOPC/DOPS have the ability to fuse onto an oppositely charged terminal layer of polyelectrolyte giving a lipid bilayer with a resistance of > 100 **kΩ**. With optical reflectometry we found that the vesicle surface charge is directly related to the amount of mass adsorbed onto the surface. An interesting observation was that zwitterionic polar head groups of DOPC allow the adsorption on both positively and negatively charged surfaces. As found with fluorescent recovery after photobleaching, positively charged surface governed by

© 2018 Manuscript version made available under CC-BY-NC-ND 4.0 license https://creativecommons.org/licenses/by-nc-nd/4.0/

the presence of poly(allylamine) as the terminal layer resulted in intact DOPC lipid vesicles adsorption whereas in the case of a negatively charged silica surface formation of lipid bilayers was observed, as expected from literature.

1. Introduction

The development of a bio-interface that mimics biological membranes is important from both the application and fundamental point of view.[1],[2],[3] Model lipid bilayers that include lipid vesicles (LVs), support-free black lipid membranes (BLM) and supported lipid bilayers (SLB) seem to be a good option to date. Over the last decade, each given example of a lipid-based bio-interface became an individual subdivision of research. Methods used most commonly for the formation of SLB include the fusion of LVs over an oppositely charged surface[4],[5] or by support decoration with the help of the Langmuir-Schaefer technique.[6] Under proper conditions, electrostatic interaction between lipid bilayer and the underlying charged support like silica,[7] TiO_2[8] or glass[9],[10] are sufficient to induce SLB formation. Direct deposition on the underlying support has a serious drawback, which is the limited space available between the membrane and the support, which may affect the fluidity of a support contacting bilayer leaflet and restricts the accommodation of functionalities like transmembrane proteins. A number of different options were proposed to overcome this problem.[11] Some examples include: (i) tethered lipid bilayers that are connected to the support via a spacer that can be covalentely bond to the support or/and lipids;[12],[13],[14],[15] (ii) formation of the lipid bilayer over self-assembled monolayers terminated with ionizable functional groups;[16] (iii) patterned surfaces that allow the formation of semi-supported lipid membranes[17] or (iv) polymeric cushions.[18]

Very elegant, fast and reproducible methods that allow the formation of polymeric cushions are based on the alternating deposition of oppositely charged polyelectrolytes.[19],[20] Layer-by-layer (LbL) formation of polyelectrolyte multilayers as a support for LB has been studied by a few groups. Although apparently an easy approach, it has resulted in a set of complex problems. Cassier *et al*. studied the formation of LB composed from phosphatidic acid or phosphatidylcholine on polyelectrolyte multilayers built up from polly(allylamine) (PAH) and polystyrene sulfonate (PSS).[21] Although LB formation was confirmed, the electric properties were indistinguishable from those measured for polyelectrolyte multilayers alone. Fishlechner *et al*. proved that the fusion of LV and the consequent LB formation is highly depending on the LV's surface charge as governed by their composition.[22] Unbeaten results

were obtained by the fusion of 1:1 (mole/mole) DOPS/DOPC LVs onto PAH terminated polyelectrolyte multilayers. Diamanti *et al.* studied the deposition of 3:7 (mole/mole) PC/PS LV onto polyelectrolyte multilayers formed from PAH and PSS.[23] An impedimetric study revealed that the lipid bilayer showed very high resistivities in order of $M\Omega cm^2$ and surprisingly high capacitance values equal to 10 – 14 $\mu F cm^{-2}$. In another report it was found that the origin of the chemical functionality of the outer polyelectrolyte layer and as a consequence the nature of interactions between support and lipids higly affects the depostion process. Moderately charged surfaces governed by the presence of an outer PAH layer together with the ability to form hydrogen bonds triggered the fusion of DOPC/DOPS LVs 1:1 (mole/mole) ratio. When the outer layer was replaced by poly(diallyldimethylammonium chloride), carrying permanently charged quaternary ammonium groups, adsorption of intact vesicles was observed.[24]

Situating the biointerface into electronic devices can mainly find applications in sensing. Potential candidates are semiconducting materials in electrolyte/insulator/semiconductor configuration. Silicon semiconductors covered with thin layer of silicon dioxide were modified with lipid bilayers using different approaches. Atansov *et al*. synthesized ether tail-containing lipids that were grafted to the surface of p-doped silica (pSi) via silane chemistry.[25] The resulting tether allowed fusion of DOPC LVs and the formation of SLB with good electrical sealing properties (in the range of $M\Omega \cdot cm^2$). Lin *et al.* used polyethylene glycol modified lipids as a polymeric cushion for the lipid bilayer (with R_{LB} in the $k\Omega \cdot cm^2$range) on single-crystal, n-doped silicon (nSi).[26] Direct fusion of dihexadecyldimethylammonium bromide LVs on pSi-surface silica layer resulted in the formation of R_{LB} in the range of $k\Omega \cdot cm^2$ that progressively increased to 1 $M\Omega \cdot cm^2$ after a few days of incubation.[27] LVs were also shown to fuse over silicon nitride/silicon dioxide covering p-doped silicon which consequently affected the electric properties of the space charge region.[28] Silicon nanowires as field-effect transistors[29] and silicon cavities[30] were also successfully modified with lipid bilayers.

The novelity of this work comes from the complexity of the system studied, i.e. an interface formed between a silicon semiconductor and a polyelectrolyte thin film, on top of which phosholipid vesicles and/or bilayer are adhered. We have employed the easiness of surface modification via a layer-by-layer depostion of polyelectrolytes on top of semiconductor devices to form charged polymeric cushion. A number of experimental variables were invesitaged in this regard:(i) the effect of silicon semicondutor doping (n or p), (ii) charge of

LVs governed by phospholipids with desired functionalites located within polar head group and (iii) the effect of polymeric cushion formed with polyelectrolytes by layer-by-layer depostion apporach. To control the surface charge of LVs we used lipids (or their mixtures) terminated with differently charged polar head groups. The electric properties of the silicon semiconductor under different bias potentials, and in the presence of polyelectrolyte layers and lipid bilayer were investigated by impedance spectroscopy. Optical reflectometry was used to study the charge dependency of the interactions between the LVs and the exposed oppositely charged polyelectrolyte layer. Using fluorescent recovery after bleaching (FRAP), we measured the lateral diffusion coefficients of lipids within the lipid bilayer formed on the bare SiO_2 and PAH. In addition to that, we were able to distinguish between lipid bilayers formed as a consequence of LVs fusion and intact adsorption of LVs.

2. Materials and Methods

2.1. Chemicals and materials

Phospholipids: 1,2-dioleoyl-3-trimethylammonium-propane chloride salt (>99%; DOTAP), 1,2-dioleoyl-*sn*-glycero-3-phospho-L-serine sodium salt (>99%; DOPS), 1,2-dioleoyl-*sn*-glycero-3-phosphocholine (>99%; DOPC), were supplied by Avanti Polar Lipids and stored in a chloroform stock solution. For FRAP experiments the Texas Red® 1,2-dihexadecanoyl-sn-glycero-3-phosphoethanolamine, triethylammonium salt (TR-DHPE) supplied by ThermoFisher was used. Polyelectrolytes: branched poly(ethyleneimine) (PEI, $\overline{\boldsymbol{M_w}}$ = 25000 g/mol, $\overline{\boldsymbol{M_n}}$ = 10000 g/mol), poly(allylamine hydrochloride) (PAH, $\overline{\boldsymbol{M_w}}$ = 17500 g/mol) and poly(sodium-4-styrene sulphonate) sodium salt (PSS, $\overline{\boldsymbol{M_w}}$ = 70000 g/mol) were all purchased from Sigma-Aldrich. The background electrolyte solutions were prepared using KCl (99%), NaCl (99%) and 4-(2-hydroxyethyl)-1-piperazineethanesulfonic acid (HEPES, ≥99.5%) were all purchased from Sigma–Aldrich. When necessary, the pH was adjusted with standard 1M solutions of HCl and NaOH from Fluka. The pH was measured using a Methrom 827 pH lab meter or with pH indicator papers. Large unilamellar vesicles LVs were prepared using the extrusion technique. Polycarbonate nucleopore track-etched membranes with 100 nm pore size were obtained from Whatman. Ø = 100 mm polyester filter supports were obtained from Avanti. Silicon wafers including n-type and p-type and covered with a 3.1 nm thick thermally grown silica layer were supplied from NXP Semiconductors (Eindhoven, The Netherlands). Gallium-indium eutectic was purchased from Alfa Aesar.

2.2. Lipid vesicles preparation

All liposomes used in this study were prepared via extrusion. First, the desired amount of lipids in chloroform were transferred into a round-bottom flask. Chloroform was evaporated under a stream of nitrogen and then the flask was kept under vacuum for at least two hours. Next, 10 mM HEPES solution was added (pH = 7.3) and the lipids were resuspended by vigorous stirring. In order to obtain large unilamellar vesicles with a narrow size distribution, the solution was extruded at least 15 times through polycarbonate membrane sandwiched between two polyester filter supports. The resulting LV solution was kept in the fridge at 4˚C and used within three weeks after preparation. Size distribution and zeta potential were measured with a Zetasizer Nano ZS from Malvern for each set of vesicles.

2.3. Polyelectrolyte multilayer formation and lipid bilayer deposition

Prior to the lipid bilayer deposition, the silicon supports were pre-treated. The protecting polymeric film was removed by rinsing using a set of solvents in the following order: 1,2-dichloromethane, isopropanol, acetone and miliQ water. The wet supports were successively dried under the stream of a nitrogen. Next, the wafers were air plasma activated for 2 min with an plasma cleaner from Harrick Plasma at pressure of 1000 mTorr and RF coil power of 29.6W. Activated samples were kept in 150 mM KCl, 10 mM HEPES (pH = 7.3) for one day before use. Polyelectrolyte multilayers were formed by alternating dipping silicon wafers in 1 mg/mL solution of PEI, PSS, PAH (and one more PSS layer in the case of DOTAP) for 30 min each, over the activated silica surface. Between each layer, the surface was thoroughly washed with 10 mM HEPES in 150 mM KCl. Lipid bilayer fabrication was performed by pipetting of 0.1 mg/mL lipid vesicle dispersion in 10 mM HEPES and 150 mM KCl on bare or polyelectrolyte-modified silica surface so that the solution covered the surface completely. After 30 min, the remaining solution was washed away making sure the lipid bilayer was hydrated all the time.

2.4.Electrochemical Impedance Spectroscopy

All impedimetric measurements were performed using an Autolab potentiostat PGSTAT302N. The three-electrode cell configuration was used as reported elsewhere.[31] An Ag/AgCl served as the reference electrode, whereas a Pt wire was used as a counter electrode. The working electrode was the silicon semiconductor connected from the backside to a copper contact plate via Indium-Gallium eutectic. Prior to the assembly, the silicon sample was scratched on the bottom side with a diamond knife to improve the ohmic contact

with the eutectic. Impedance spectra were recorded in the frequency range from 100 $\boldsymbol{kHz}$ down to 100 $\boldsymbol{mHz}$, with an amplitude $\boldsymbol{E_{ac}}$ equal to 10 $\boldsymbol{mV}$ with an integration time of 0.125 $\boldsymbol{s}$. During the measurements, the superposed bias voltage was varied between +0.6 $\boldsymbol{V}$ and –0.6 $\boldsymbol{V}$ allowing the control of charge distribution in the space charge region. All measurements were performed in 10 mM HEPES with 150 mM KCl. Prior to each experiment, the silicon wafers were air plasma treated for 2 $\boldsymbol{min}$. and incubated overnight in the background electrolyte solution.

2.5.Zeta potential and size distribution measurements

Zeta (ζ) potential and size distribution measurements of the lipid vesicles were performed at 20˚C with a ZetaSizer NanoZS instrument from Malvern. The instrument calculated the ζ-potential based on the electrophoretic mobility of liposomes according to Smoluchowski approximation.[32] The reported ζ-potentiala are an average of 15 consecutively repeated scans. Size distribution of the lipid vesicles was determined based on dynamic light scattering (DLS) phenomena and the ζ-potential was calculated by the Malvern software. The average sizes of lipid vesicles together with corresponding ζ-potentials are given in Table 1. All measurements were performed in 10 mM HEPES in 150 mM NaCl.

Table 1. Z-average sizes and ζ-potentials of lipid vesicles composed from different lipids.

Lipid composition	**DOPC***	**DOPS***	**DOPC/DOPS* (1:1 mole:mole)**	**DOTAP***
⌀ / nm	128.7 (+/– 5.0)	110.3 (+/– 1.5)	115.0 (+/– 5.0)	97.5 (+/– 2.3)
ζ-potential / mV	–5.0 (+/– 0.2)	–41.8 (+/– 1.0)	–22.0 (+/– 2.0)	43.8 (+/– 0.9)

* Errors are calculated based on three independent measurements. Polydispersity index was found in the range from 0.050 to 0.090 indicating monomodal and highly monodispersed samples.

2.6. Fixed angle stagnation point optical reflectometry

The polyelectrolyte multilayer and lipid bilayer deposition on silica surfaces were studied with the fixed angle, stagnation point optical reflectometry (OR).[33] The idea behind this technique is to relate a reflected light signal to the amount of adsorbed material, by measuring changes in the parallel (I_p) and perpendicular (I_s) polarized light intensities upon adsorption:

$$\boldsymbol{S = \frac{I_p}{I_s}} \tag{1.1}$$

The change in the signal *S* indicates the adsorption at the solid – liquid interface as the refractivity of the surface alters. Surface excess (Γ) of the adsorbate can be defined and related to *S* by:

$$\boldsymbol{\Gamma = \frac{S - S_0}{S_0} Q_f} \tag{1.2}$$

where S_0 is the signal reflected from the bare silica surface, *S* is the signal recorded after adsorption and Q_f is the inverse of a sensitivity factor. Determination of the latter requires the knowledge of reflectivities of silicon, silica and adsorbed layers. We used dedicated software (prof. Huygens, version 1.2C Dullware) with the following parameters: thickness of silica layer $\boldsymbol{d_{SiO_2}}$= 70 nm; refractive index of silica $\boldsymbol{n_{SiO_2}}$= 1.46; refractive index of silicon $\boldsymbol{n_{Si}}$ = 3.85; refractive index of the solution $\boldsymbol{n_{solution}}$= 1.33, laser wavelength $\boldsymbol{\lambda}$ = 632.8 nm and $\boldsymbol{dn/dc_{PEI}}$ = 0.176 $\boldsymbol{mL/g}$[34] to calculate the mass of the first polyelectrolyte layer – PEI. Unfortunately the $\boldsymbol{dn/dc}$ increment for subsequent polyelectrolytes and LVs are unavailable. For lipid bilayers we used a value of $\boldsymbol{dn/dc_{LB}}$ = 0.146 $\boldsymbol{mL/g}$ reported for DOPC/DOPG system.[35] Consequently instead of giving mass uptake we used relative signal increase to interpret surface adsorption process, as it is common practise in OR measurements. Before each experiment, the silica surface was treated with an air plasma to remove ubiquitous organic contaminations and to activate the surface by the formation of extra silanol species resulting in a high surface density of these groups.

The optical reflectometer used in this study is a custom-built instrument from Fijn-Mechanische Werkplaats, Wageningen, The Netherlands. For the support, we used nSi wafers with a 70 nm thick thermally grown silica layer. Before each experiment started, the wafers were cleaned using acetone and miliQ water, followed by N_2 drying. Activation of a surface was completed by an air plasma treatment for 120 sec.

2.7.Fluorescent Recovery after Photobleaching

The mobile fraction, lateral diffusion coefficients of lipids as well as mechanistic information originating from the interaction between lipids and underlying support were studied using FRAP. For these measurements, LV with desired ratios of the main lipids were doped with 0.5 mol% of the lipid conjugated fluorescence dye TR-DHPE were prepared. These LV were

incubated at a concentration of 0.1 mg/mL on glass substrates that were pre-activated with 1M NaOH for 1h and rinsed copiously with Milli-Q water. After 30 minutes incubation and subsequent carful rinsing, the FRAP measurement was performed using a confocal microscope (Nikon A1 CSLM), using a 561 laser and 570-620 emission filter. The protocol consisted of 11 imaging loops (1 second interval) before bleaching in order to establish a baseline, then 5 loops of bleaching with 100 % laser intensity and with no delay in between loops (giving a total time of 1.19 seconds) and either 300 or 600 loops of recovery (1 second interval). The intensity is normalized and corrected for acquisition bleaching by using the fluorescence intensity in a location not too close to the bleach spot. The bleach spot was 10 µm in diameter. FRAP curves were fitted with the modified Bessel functions as described by Soumpasis *et al*.[36] FRAPAnalyser (University of Luxembourg) was used for the fitting to determine the diffusion constant and the degree of recovery.

3. Results and discussion

3.1. Optical reflectometry

First, we investigated the polyelectrolyte adsorption followed by LV addition with an optical reflectometry. The $\boldsymbol{pK_a}$ of a silica[37] equals to 4 – 4.3; for PEI[38] $\boldsymbol{pK_a}$ values can be found in the range from 8 to 11, for PAH[39] $\boldsymbol{pK_a} \approx 8.5$ whereas PSS[40] is a strong polyelectrolyte ($\boldsymbol{pK_a} \approx 1$) that holds a negative charge in an almost full pH range. Consequently, to ensure charge reversal between support and each added layer we worked at fixed pH = 5.5. The representative experiment showing signal evolution in time for a polyelectrolyte multilayer composed from PEI followed by 17 layers formed via alternating addition of PSS and PAH is shown in Figure S1. PEI is commonly used as the first layer since it holds a positive charge in a wider pH range as compared to PAH. For the given background electrolyte concentration of [NaCl] = 150 mM we found a linear build-up of the signal that is indicative of the corresponding ionic strength.[41],[42] At higher background electrolyte concentrations, *i.e.* higher ionic strengths, the signal originating from multilayer build-up grows exponentially.[41],[42] After each polyelectrolyte addition, the modified support was flushed for at least 100 sec. with 150 mM NaCl (pH = 5.5) and as it is shown in Figure S1 and Figure 1A no significant changes in signals are observed. This means that no delamination of terminal layers occurred. The signal increase upon the adsorption of the first three layers composed of PEI, PSS and PAH was equal to 0.020 (+/– 0.005), 0.023 (+/– 0.006) and 0.024 (+/– 0.008), respectively, and was determined from four independent experiments. Using Eq.

1.2 with Q_f = 26 we calculated the adsorbed mass to be equal to 0.56 mg/m^2 for PEI which correlates well with 0.69 mg/m^2 reported for PEI at pH = 5.5 and [NaCl] = 150 mM[42] or 0.40 mg/m^2 for PEI measured at pH = 5.8 and [NaCl] = 100 mM.[43] As the d*n*/d*c* for other polyelectrolytes is not available we could not calculate the surface mass uptake. Consequently, for comparative purposes, we focused on the relative signal increase. The optical reflectometry signal recorded after the addition of the LVs having different composition and consequently different surface charges to the polyelectrolyte cushion is shown in Figure 1A. For the DOPC, DOPS and DOPC/DOPS the outermost (top) polyelectrolyte layer was PAH, whereas for DOTAP it was PSS. In all cases, the addition of the LVs resulted in a signal increase which was one order of magnitude larger as compared with the polyelectrolyte adsorption. The relative signal increments equals to 0.504 for DOPC, 0.178 for DOPS, 0.290 for DOPC/DOPS and 0.191 for DOTAP. As shown in Figure 1C these values correlate well with the measured absolute values of the zeta potential of LVs in the bulk phase. This indicates that the interaction between support and LVs are very much governed by electrostatics. At this point, we speculate that the LVs composition and consequent surface charge governs the morphological surface properties of the adsorbed bilayers resulting in three scenarios as shown in Figure 1D. (i) The highest signal increase found after addition of DOPC LVs, that reached steady state after around 350 sec., can be attributed to adsorption followed by the organization of intact LVs. The low value of the surface potential (ζ = –5 $\boldsymbol{mV}$) and the possibility to induce orientation of zwitterionic polar head groups of DOPC[44],[45] allows the formation of a compact layer of intact LVs. (ii) As reported by others,[22],[24] and proved in the following sections of this paper the LVs composed from 1:1 (mole:mole) mixture of DOPC/DOPS fuse over oppositely charged PAH layer and form a lipid bilayer. With the value of $\boldsymbol{dn/dc}$ = 0.146 mL/g reported for DOPC/DOPG[35] we calculated that the relative signal increase $(\boldsymbol{S-S_0})/\boldsymbol{S_0}$ = 0.290 corresponds to ca. 10 mg/m^2 of a lipids at the surface. Assuming a surface area ($\boldsymbol{a}$) per lipid ($\boldsymbol{a_{DOPC}}$ = 0.73 nm^2 and $\boldsymbol{a_{DOPS}}$ = 0.65 nm^2),[46] lipids molar mass ($\boldsymbol{M_{DOPC}}$ = 786.11 g/mol and $\boldsymbol{M_{DOPS}}$ = 810.25 g/mol) and homogeneous 1:1 distribution of the lipids within the bilayer, we calculated theoretical surface excess equal to 3.85 mg/m^2. In addition to the $\boldsymbol{dn/dc}$ increment that can deviate for our lipid composition we can speculate that the discrepancy between theoretical and measured values (3.85 *vs.* ~10 mg/m^2) indicates that a higher specific surface area, induced by the roughness of the polyelectrolyte cushion, is available for lipids, which can be translated into higher signal increase. (iii) For the LVs with highest surface charge, *i.e.* DOPS (ζ = –41.8 $\boldsymbol{mV}$) and DOTAP (ζ = 43.8 $\boldsymbol{mV}$), in addition to the strong surface

adsorption that constrains their fusion, we anticipate some spacing to occur between intact LVs due to electrostatic repulsion. The resulting layer is expected to be mass depleted as compared with DOPC, which result in a lower signal.

The findings derived from OR measurements are in agreement with the EIS and FRAP data as will be discussed in following sections.

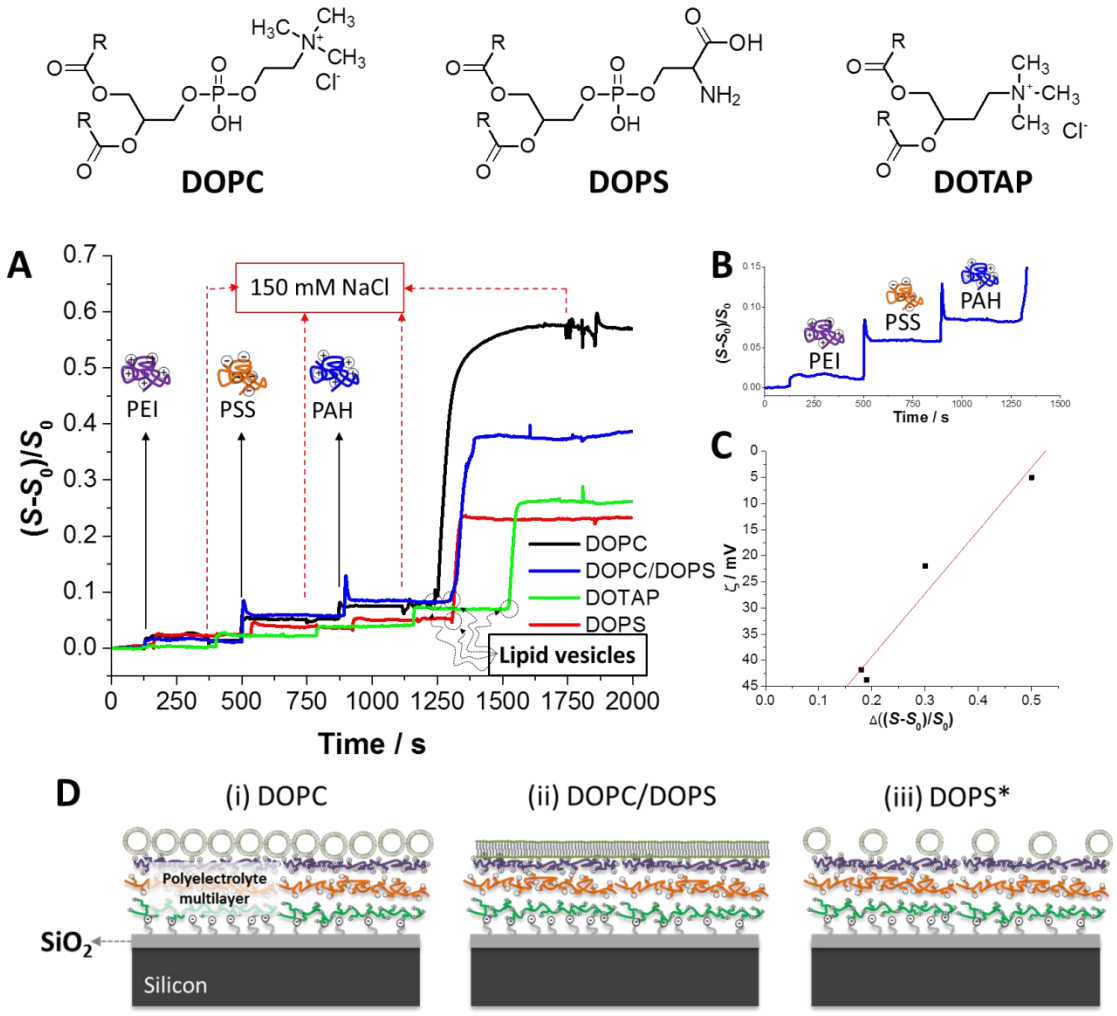

Figure 1. A – Optical reflectometry signal for the polyelectrolyte multilayer build-up terminated by the addition of LVs. Black-solid arrows indicate the addition of three first layers of polyelectrolytes (in the case of DOTAP, a fourth layer of PSS was deposited). Red-dashed arrows correspond to 150 mM NaCl flushing step. Concentration of polyelectrolytes was 1 mg/mL at pH ≈ 5.5. Concentration of lipid vesicles was 0.1 mg/mL at pH = 7.3; B – zoom in into the optical reflectometry signal originating from polyelectrolyte adsorption prior to DOPC/DOPS LVs addition; C – Absolute value of zeta potential measured for lipid vesicles at pH = 7.3 as a function of relative reflectometry signal increase measured after last

polyelectrolyte layer deposition; D – Schematic representation (not to scale) of the LVs at different lipid compositions deposited on polyelectrolyte cushion: (i) densely packed intact lipid vesicles; (ii) lipid bilayer originating from fused lipid vesicles and (iii) loosely packed lipid vesicles (*DOTAP LVs are expected to adsorb in the same manner as DOPS onto PSS as the terminal layer). Chemical structures of the lipids can be found on top of the figure (R stands for 9Z-octadecanoyl substituent).

3.2.Electrochemical Impedance Spectroscopy

3.2.1. The impedance of the electrolyte – unmodified SiO_2 – silicon semiconductor

Impedance spectroscopy is routinely used to study electrolyte – insulator – semiconductor interfaces.[47],[48],[49] The electric properties of the semiconductor can be affected by application of an external bias polarization or by the changes in the surface charge density. Both will affect the valence and conductance band bending in the space charge region. For n-doped Si the majority charge carriers are electrons. By definition, the external potential at which the net transfer of charge is equal to zero is called flat-band potential ($\boldsymbol{E_{fb}}$). At potentials more negative than $\boldsymbol{E_{fb}}$ the electrons are accumulated in the space charge region and the impedance of a system is governed by a purely capacitive behaviour of the thin silica layer in series with the resistance of the electrolyte (Figure 2A). At potentials more positive than $\boldsymbol{E_{fb}}$ the electrons are depleted from the space charge which adds additional *RC* time constant to the equivalent circuit (Figure 2B).

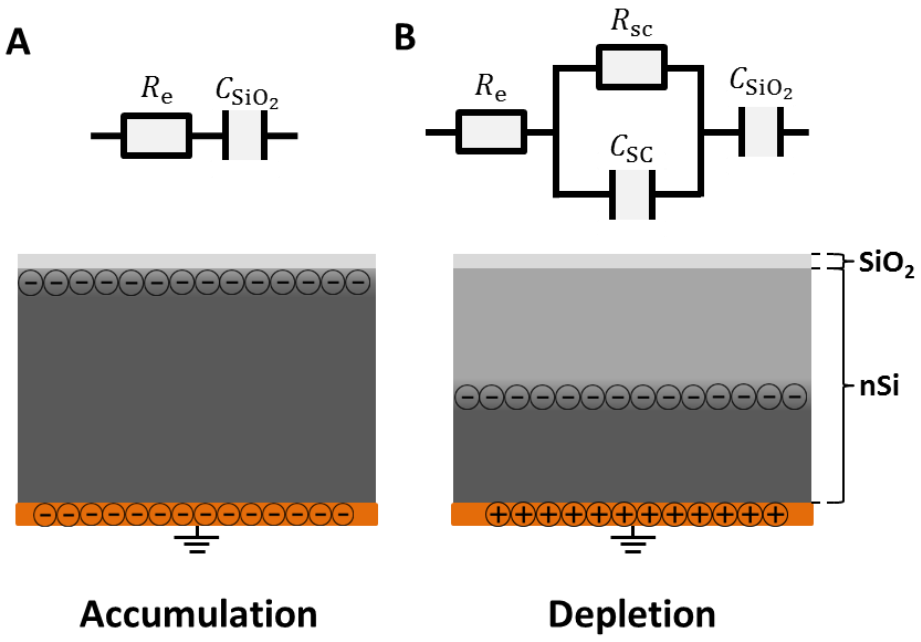

Figure 2. Schemes of n-doped Si under accumulation (A) and under depletion (B) and corresponding equivalent circuits used for impedance spectra fitting.

Bode phase plots (Bode modulus plots can be found in Figure S2) for nSi semiconductor in 10 mM HEPES and 150 mM KCl (pH = 7.3) at different applied bias potentials *vs.* the Ag/AgCl reference electrode are shown in Figure 3A. Under negative potential ($E < -0.4$ V) the silicon semiconductor is under full accumulation and the phase shift in the low and medium frequency reaches almost –90˚, which is governed by the purely capacitive behavior of the silicon oxide surface layer ($\boldsymbol{C_{SiO_2}}$). The phase shift at high frequency approaches 0˚ and represents the resistance of the electrolyte. As the bias potential is gradually increased towards more positive values the space charge region is progressively depleted from the negative charge carriers. This depletion can be translated into time constant (*RC*) as represented by the parallel space charge resistance ($\boldsymbol{R_{SC}}$) and capacitance ($\boldsymbol{C_{SC}}$). Impedance spectra recorded at intervals of 0.1 V in the range from –0.7 to –0.5 V were fitted with the equivalent circuit from Figure 2A. Plots recorded from –0.4 to +0.7 V were fitted using equivalent circuit from Figure 2B. Results of the fittings are given as $\boldsymbol{1/C_{SC}^2}$ (Figure 3B) and $\boldsymbol{R_{sc}}$ (Figure 3C) as a function of applied potential. At a bias potential lower than –0.4 V nSi was under full accumulation and only $\boldsymbol{C_{SiO_2}}$ = 250 (+/– 24) $\boldsymbol{nF \cdot cm^{-2}}$ was obtained from our fitting based on the average of more than ten independent experiments. At $+0.4 \geq E \geq +0.7$ V the depletion layer was relatively unaffected by the applied potential, reaching its maximum $\boldsymbol{R_{SC}}$ equal to few $\boldsymbol{M\Omega}$ and $\boldsymbol{C_{SC}}$ equal to a few $\boldsymbol{nF}$. When the potential approach the $\boldsymbol{E_{fb}}$ of nSi the steep variation ranging over a few orders of magnitude for both components were observed.

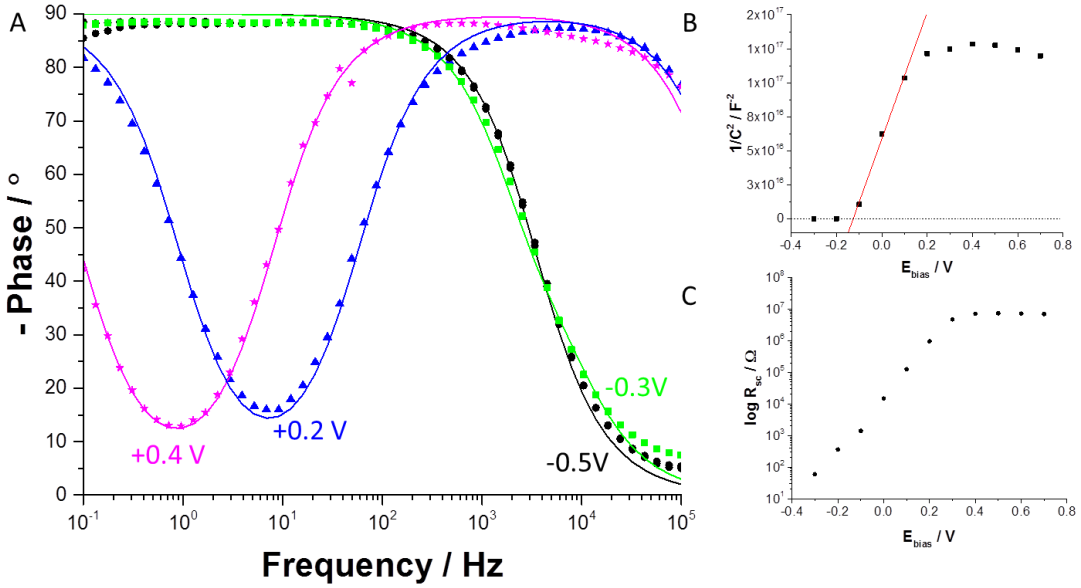

Figure 3. A – Bode plots for the nSi recorded at different bias potential in 10 mM HEPES in 150 mM KCl at pH = 7.3. Black circles E = –0.5V; green squares E = –0.3V; blue triangles E = +0.2V and violet stars E = +0.4V. The best fit is given with solid lines. All bias potentials were recorded *vs.* an Ag/AgCl reference electrode. B – Mott-Schottky plot giving space charge region capacitance as a function of applied bias potential and C – resistance of the space charge region in function of applied bias potential. Capacitance and resistance values were obtained from impedance data fitting using equivalents circuits from Figure 2.

The flat-band potential for nSi as obtained from the Mott-Schottky dependency was about –0.13V. By analogy, the p doped Si semiconductor gives inverse behavior as the majority charge carriers are here the positively charged holes. Impedance spectra together with the fitting parameters for pSi are given in Figure S3. The flat-band potential for pSi in 10 mM HEPES and 150mM KCl (pH = 7.3) was around +0.03V. Similar observations and findings are documented and can be found in the literature.[31],[47],[48]

3.2.2. Impedance of lipid bilayers on bare silicon semiconductor

No changes in the impedance were observed after the addition and incubation of lipid vesicles composed of DOPS, DOPS/DOPC and DOTAP to bare SiO_2 – silicon semiconductor. For the first two systems this is not surprising, as the solution pH equals 7.3, assuring the silica surface to be negatively charged, which in consequence electrostatically repels DOPS and

DOPS/DOPC lipids vesicles with the measured zeta potential equal to –41.8 $\boldsymbol{mV}$ and –22 $\boldsymbol{mV}$ respectively. However, the quaternary ammonium cation being exposed to the exterior of DOTAP lipid vesicles provided a net positive charge of +43.8 $\boldsymbol{mV}$. Also, in that case, we did not observe any change in the impedance spectra within studied frequency range. As already concluded when discussing the OR results, the DOTAP LVs adsorption over negatively charged PSS layer or as it is in the case of bare silica surface, can show voids between intactly adsorbed vesicles. Since the electrical current will certainly pass through such a configuration we cannot anticipate the formation of a resistive layer. It is very interesting to note that changes in the impedance and phase shift were observed after the addition of lipid vesicles composed of DOPC to the bare SiO_2 – silicon semiconductor surface. At given pH = 7.3, the measured zeta potential of the lipid vesicles from DOPC was always slightly negative and equal to around – 5 $\boldsymbol{mV}$. Consequently, one would expect that the net negative surface charges should repel each other which is not the case here. It was found that the orientation of the choline head group within the lipid bilayer (or monolayer) framework is highly affected by the composition of the contacting solution, including the pH.[50],[51] At neutral pH both the positively charged quaternary ammonium cation being part of a choline moiety and the phosphate functionality situated within the polar head group are expected to be oriented parallel to the plane of a bilayer. What might happen when these vesicles approach the silica surface, is that the lipid polar head groups orientation might change. The exposed quaternary ammonium cation might orient to the deprotonated silanol groups which in turn now enables adsorption followed by fusion. Figure 4 shows the phase shift as a function of applied frequency for nSi (Figure 4A) and pSi (Figure 4B) under accumulation conditions. The applied bias potential was $\boldsymbol{E_{DC}}$ = –0.4 V for nSi and $\boldsymbol{E_{DC}}$ = +0.4 V for pSi. As predicted from our simulations (see supporting information) the emergence of an *RC* time constant attributed to a lipid bilayer with moderate resistance can be observed in the region from 10 to 10^3 $\boldsymbol{Hz}$.

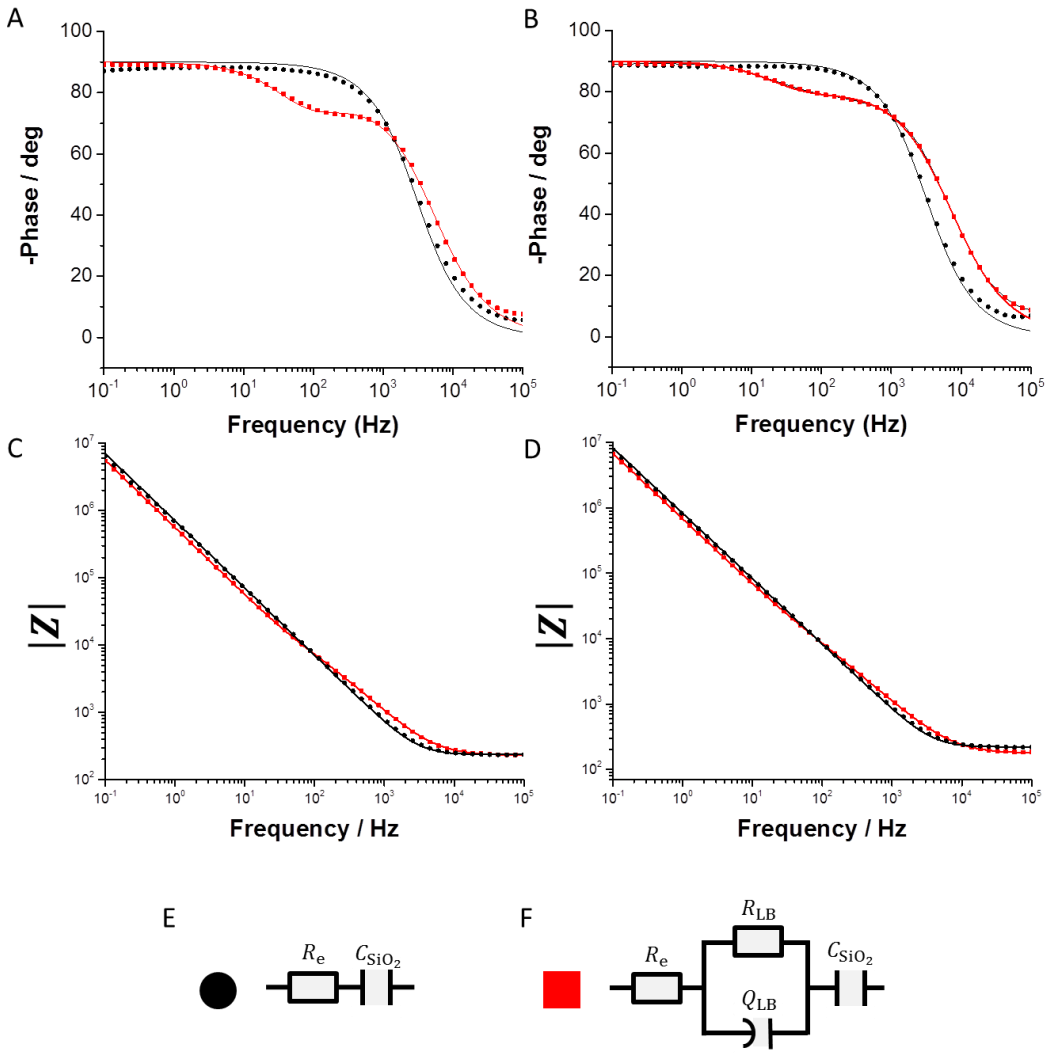

Figure 4. Phase shift (A,B) and total impedance (C,D) as function of the frequency for A, C – nSi with a bias potential of $\boldsymbol{E_{DC}}$ = +0.4 V and B, D – pSi with a bias potential of $\boldsymbol{E_{DC}}$ = –0.4 V. Black circles correspond to the unmodified surface, red squares were recorded after DOPC vesicle fusion. Solid lines correspond to fitting performed with the equivalent circuits depicted in E (before modification) and F (after modification).

Bode plots recorded prior to the lipid bilayer deposition were fitted using a simple circuit given in Figure 4E where the resistance of the electrolyte and connections are in series with the capacitance of the thin silica layer. The presence of the LB adds an *RC* time constant to the circuit as it is shown in Figure 4F. For the latter fitting was performed with C_{LB} and constant phase element (CPE). The latter was used to indicate inhomogeneity of lipid bilayers. The results of the fitting are summarized in Table 2 and were found to be indicative for an

SLB that is not free from electrical defects as (i) the measured range of the resistivities remains at relatively low level, *i.e.* from 0.38 to 1.06 $k\Omega \cdot cm^2$ and (ii) better fitting results were obtained in the presence of CPE with an n exponent value of about 0.80.

Table 2. Fitting parameters of a lipid bilayer formed over nSi and pSi.

Doping type	R_{LB} / $k\Omega \cdot cm^2$	C_{LB} / $\mu F \cdot cm^{-2}$	Q / µS	n
nSi	1.06 (+/– 0.05)	–	2.29 (+/– 0.01)	0.79
	0.38 (+/– 0.02)	1.80 (+/–0.01)	–	–
pSi	0.80 (+/– 0.06)	–	1.35 (+/–0.09)	0.84
	0.47 (+/– 0.01)	0.85 (+/– 0.10)	–	–

Similar experiments were repeated a few times and showed that the resistance values of a SLB remain within the $k\Omega \cdot cm^2$ range for both n- and p-doped silicon supports. R_{LB} was found to increase slightly after few days of incubation, although it still stayed within the same order of magnitude. What is very interesting is the observation that for pSi semiconductors we were constantly recording significantly lower capacitance values as compared to nSi semiconductors. Expected values of a normalized capacitance of a black lipid membrane are usually found in the range from 0.3 – 1 $\mu F \cdot cm^{-2}$ depending from lipid bilayer composition and physicochemical properties of the contacting solution.[52],[53],[54] Fitting revealed that the C_{LB} values of the SLB formed on pSi fall into this range as it equals to 0.85 $\mu F \cdot cm^{-2}$ whereas it was twice a high – 1.80 $\mu F \cdot cm^{-2}$ – when nSi was used a support. As the change in a surface charge of a thin silica layer can affect the thickness of the space charge region, so can the external polarization change apparent dissociation constant of a surface silanol groups. We speculate here that at +0.4 V applied as a bias potential to ensure accumulation of an nSi the net negative charge of a silica surface was much higher as compare to pSi that was kept at –0.4 V. Following the same reasoning we can expect stronger interactions between both the outer and the inner leaflets of an SLB and the surface of nSi. This can be proved by simple scrutiny. We can consider the lipid bilayer as a planar parallel plate capacitor of which the capacitance is defined by:

$$C_{LB} = \frac{\varepsilon \varepsilon_0 A}{d} \tag{1.3}$$

where $\boldsymbol{C_{LB}}$ is the capacitance of a lipid bilayer, $\boldsymbol{A}$ is the electroactive surface area, $\boldsymbol{\varepsilon}$ stands for the dielectric constant of the interior of lipid bilayer, which is usually taken to be 2 – 2.2,[55],[56] $\boldsymbol{\varepsilon_0}$ is the relative permittivity of vacuum ($8.854 \cdot 10^{-12}$ $\boldsymbol{F \cdot m^{-1}}$) and *d* is the thickness of lipid bilayer. As the dielectric constant remains intact, with the normalized capacitance values obtained from the fitting we can easily calculate the thickness of an SLB that falls in the range from 2.1 nm to 2.3 nm for 0.85 $\boldsymbol{\mu F \cdot cm^{-2}}$ and from 1.0 nm to 1.1 nm for 1.80 $\boldsymbol{\mu F \cdot cm^{-2}}$. These values hold the same order of magnitude as the expected 4 to 5 nm frequently found in literature.[57] This difference of a factor of 2 – 4 can be related to a stronger interactions between the charged head group located within upper lipid bilayer leaflet that may (i) induce orientational changes of polar head groups, (ii) increase the mutual penetration of alkyl chains or (iii) cause the tilt of phospholipids towards the plane of a support surface. The pseudo capacitance calculated from fitting when CPE was used instead of $\boldsymbol{C_{LB}}$ and can be derived using following formula:

$$\boldsymbol{C_{pseudo,LB} = Q^{\frac{1}{n}} \cdot R^{(\frac{1}{n}-1)}} \quad (1.4)$$

Where *Q* and *n* are the admittance and the exponent of a CPE and *R* is the resistance connected in parallel. Although calculated values of pseudo-capacitance were found to be relatively high, *i.e.* ~3.6 $\boldsymbol{\mu F \cdot cm^{-2}}$ for LB at nSi and ~2.6 $\boldsymbol{\mu F \cdot cm^{-2}}$ for LB deposited at pSi, we can still observe the same tendency.

3.2.3. Impedance study after deposition of polyelectrolytes and lipid bilayers

The resistivity and capacitance of the polyelectrolyte multilayers reported by others were found to be dependent on the resulting film thickness and type of the polymers used.[58],[59],[60] For PSS/PAH, reported values of resistivity of the multilayers increased from a few $\Omega \cdot cm^2$ at the initial stage of multilayer formation up to few $k\Omega \cdot cm^2$ for thick films, whereas the capacitance values were found in the range of 7.7 to 9.6 $\mu F \cdot cm^{-2}$.[58] These values were obtained using a model that assumes (i) an incomplete surface coverage with the formation of pinholes at the initial stage of multilayer formation and (ii) complete coverage of the electroactive surface area for thick multilayers. Irrespectively from the number of layers deposited, we never observed any change in impedance spectra after polyelectrolyte deposition under both accumulation (see Figure S7) and depletion conditions. This is due to the fact that the smallest capacitance value governs the overall capacitance, and

since C_{PEM} with relatively small R_{PEM} is expected to be two order of magnitude higher than $C_{\mathrm{SiO_2}}$ the impedance at medium and lower frequency range will be governed by the latter.

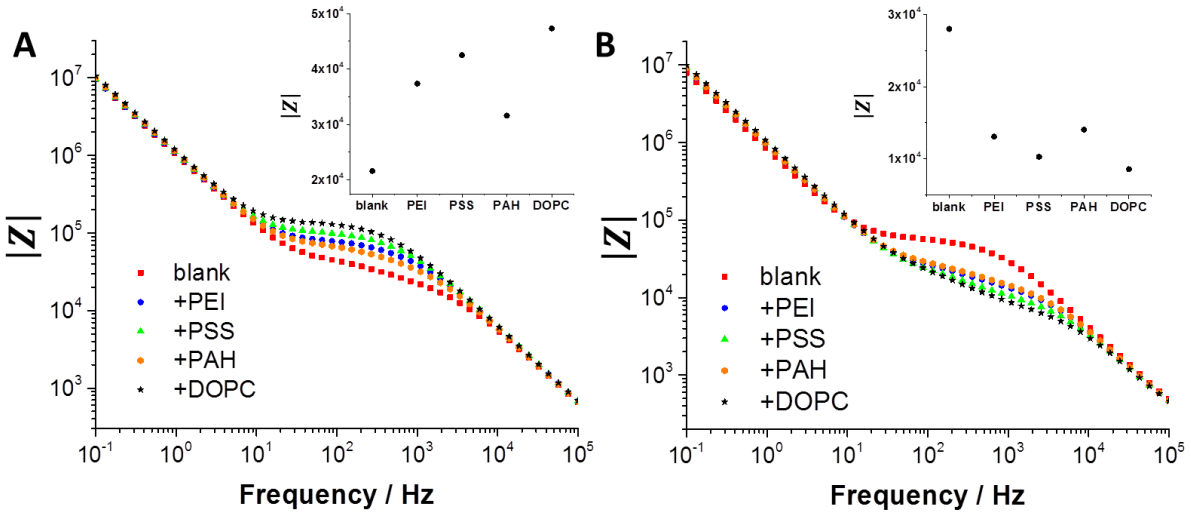

Figure 5. Bode plots for A – nSi at $\boldsymbol{E_{DC}}$ = +0.1 V and B – pSi at $\boldsymbol{E_{DC}}$ = –0.1 V recorded after sequential deposition of polyelectrolytes terminated with adsorption of DOPC lipid vesicles. The insert of both graphs corresponds to the total impedance recorded at 153 $\boldsymbol{Hz}$ as a function of the deposited layer. All graphs were recorded in 10 mM HEPES, 150 mM KCl. Bias potential was applied *vs.* Ag/AgCl reference electrode.

The adsorption of charged species to the silica surface could only be followed at bias potentials assuring a weak depletion. Under such conditions, the thickness of the space charge region can be very much influenced by the variation of the surface potential. Adsorption of polyelectrolytes followed with field effect-devices, where the surface potential[61],[62],[63] or space charge region capacitance[31] is plotted against the charge of the adsorbate, gives characteristic zig–zag patterns. For our system, the effect of polyelectrolytes and LVs added to the SiO_2 – silicon semiconductor interface is shown in Figure 5 in a form of total impedance ($|\boldsymbol{Z}|$) as function of the applied frequency. For the frequency region of 10^4 to 10^1 $\boldsymbol{Hz}$ we observed very reproducible patterns. The $|\boldsymbol{Z}|$ measured at 153 $\boldsymbol{Hz}$ for nSi (Figure 5A, insert) increased from 21.6 $\boldsymbol{k\Omega}$ for the first two layers, namely PEI to 37.4 $\boldsymbol{k\Omega}$ and PSS to 42.5 $\boldsymbol{k\Omega}$. Third layer, caused $|\boldsymbol{Z}|$ to decreased down to 31.6 $\boldsymbol{k\Omega}$ and was further increased to 47.3 $\boldsymbol{k\Omega}$ after DOPC LVs addition. As we have not observed any changes in the impedance spectra for nSi hold under accumulation (E_{DC} = –0.4 V) upon addition of DOPC LVs we

concluded that intact LVs are adsorbing to the terminal polyelectrolyte layer rather than a lipid bilayer is formed.

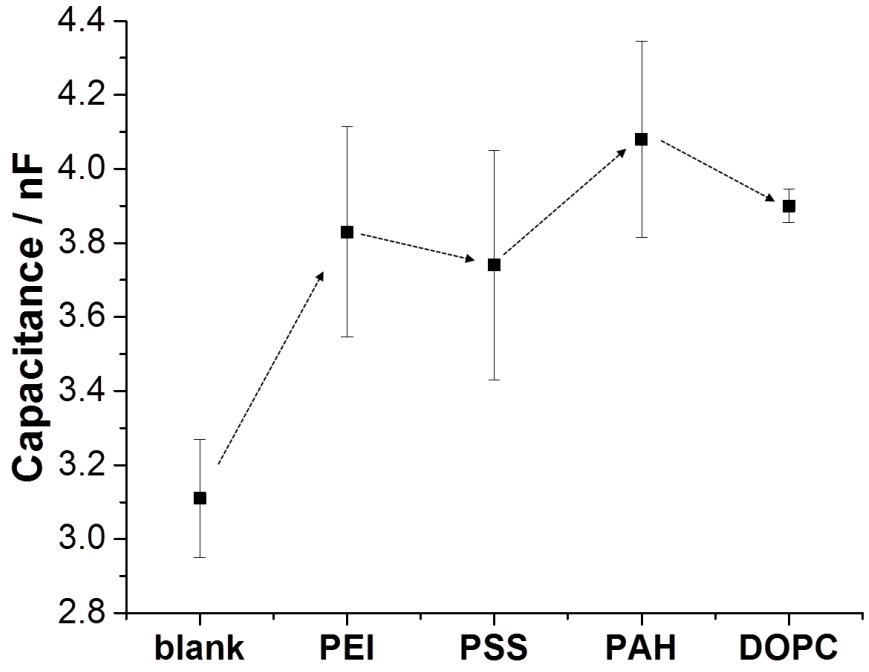

Figure 6. The capacitance of a space charge region of nSi was measured at E_{DC} = +0.1 V after subsequent addition of polyelectrolytes and DOPC lipid vesicles. All values were obtained with the equivalent circuit from Figure 4 assuming $\boldsymbol{R_{LB}}$ and $\boldsymbol{C_{LB}}$ = 0. Error bars are calculated based on three independent experiments. The arrows are a guide for ther eye.

Mirror-like patterns were obtained for the pSi as depicted in Figure 5B. In order to have a deeper understanding of what is happening within the space charge region upon adsorption of charged species, we extracted $\boldsymbol{R_{SC}}$ and $\boldsymbol{C_{SC}}$ by fitting the data from Figure. 5A to the equivalent circuit from Figure S4. We assumed that DOPC LVs form a monolayer of intact LVs with a high density of electrical defects; this way we ignore any contribution of $\boldsymbol{R_{LB}}$ and $\boldsymbol{C_{LB}}$. C_{SC} as function of adsorbents with alternating charge deposited over the SiO_2 – nSi interface is shown in Figure 6. Since for nSi the majority charge carriers are electrons, it is not surprising that in the presence of the first layer – PEI – the C_{SC} increases from 3.1 $\boldsymbol{nF}$ to 3.8 $\boldsymbol{nF}$. This effect can be explained by negative surface charge screening that consequently enlarges the attraction of the electrons towards the surface and diminishes the thickness of the

space charge region. The addition of PSS resulted in a C_{SC} drop to 3.7 nF (increased charged repulsion) whereas for PAH it increased to 4.1 **nF** (charge screening). Finally, under given experimental conditions we could electrochemically detect the adsorption of DOPC LVs as the C_{SC} decreased to 3.9 **nF**. The exact mechanism related to surface charge turnover is not known, but it probably consists of a few effects: (i) as the observed C_{SC} was highest after first layer deposition we anticipate that the change of a surface charge is escalated due to protonation of a negatively charged (*i.e.*, deprotonated) silanol groups and introduction of amine functionalities with a net positive charge. In addition to (ii) purely electrostatic interactions between alternatively charged polyelectrolytes we cannot exclude the (iii) variation in local pH affected by uptake or release of a proton (that can diffuse across the multilayer)[64] by ionisable functionalities and (iv) release of counterions from the polyelectrolyte film affecting local ionic strengths. The impedance of silicon semiconductors held at bias potential assuring weak depletion of a space charge region revealed the adsorption of other the LVs (*i.e.*, DOPS and DOTAP), that did not fuse over the oppositely charged terminal layer of polyelectrolyte.

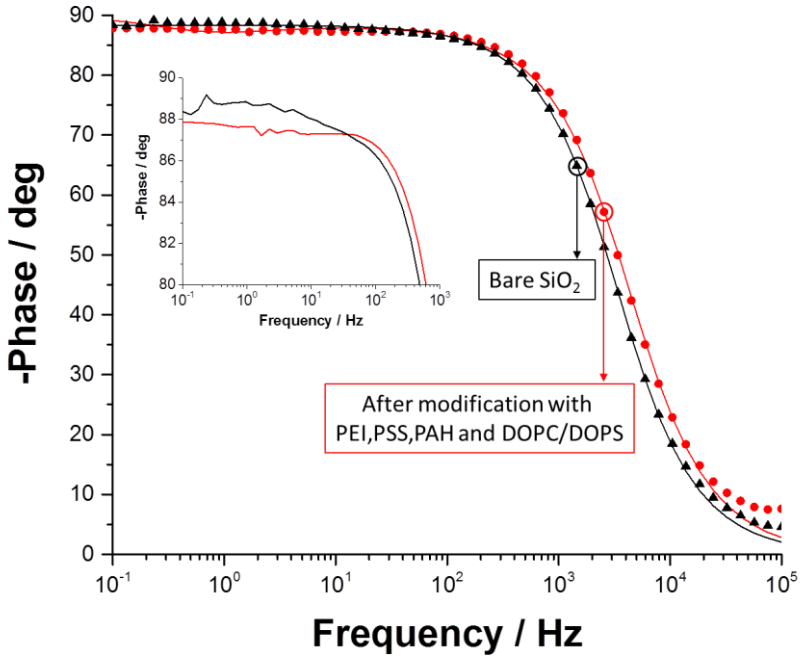

Figure 7. Bode phase recorded for bare SiO_2 (black) and after deposition of PEI, PSS, PAH and DOPC/DOPS (red). Both spectra were recorded for nSi hold at bias potential E_{DC} = –0.4V in 150 mM KCl and 10 mM HEPES. Experimental data were fitted using equivalent

circuit from Figure 4 ($\boldsymbol{R_{SC}}$ and $\boldsymbol{C_{SC}}$ = 0). Insert shows zoom into experimental data where the inflection point indicating the presence of lipid bilayer occurred. Due to small change in total impendace, Bode modulus plots are not show.

Bode phase plots recorded before and after deposition of three polyelectrolyte layers (PEI, PSS and PAH) followed by the addition of DOPC/DOPS LVs are shown in Figure 7. As the shape of the impedance spectra barely changed after deposition of polyelectrolytes we show only the one that was recorded after addition of DOPC/DOPS LVs. We observed the evolution of a very shallow inflection point (Figure 7, insert) between 1 $\boldsymbol{Hz}$ and 10 $\boldsymbol{Hz}$ that, based on our simulation (see supporitng information), can be attributed to the formation of a lipid bilayer with high capacitance and moderate resistivity. Indeed, using the equivalent circuit from Figure S4 (with $\boldsymbol{C_{SC}}$ and $\boldsymbol{R_{SC}}$ = 0 and $\boldsymbol{C_{PEM}}$ and $\boldsymbol{C_{LB}}$ replaced with constant phase elements) with predefined electrical properties of polyelectrolyte multilayer ($\boldsymbol{R_{PEM}}$ = 10 $\boldsymbol{k\Omega cm^2}$ and $\boldsymbol{C_{PEM}}$ = 5.1 $\boldsymbol{\mu F cm^{-2}}$) we obtained the electric properties of a lipid bilayer that are listed in Table 3.

Table 3. Electrical parameters of a DOPC/DOPS lipid bilayer and polyelectrolytes (PEI, PSS and PAH) obtained from fitting the impedance spectra shown in Figure 9

$\boldsymbol{R_e}$ / $\boldsymbol{\Omega}$	*$\boldsymbol{R_{PEM}}$ / $\boldsymbol{\Omega cm^2}$	*$\boldsymbol{C_{PEM}}$/ $\boldsymbol{\mu F cm^{-2}}$	$\boldsymbol{R_{LB}}$/ $\boldsymbol{k\Omega cm^2}$	$\boldsymbol{Y_{LB}}$ / $\boldsymbol{\mu F cm^{-2} s^{n-1}}$	$\boldsymbol{n_{LB}}$	$\boldsymbol{C_{SiO_2}}$ /$\boldsymbol{\mu F cm^{-2}}$
216	10	5.1	36.1	4.07	0.78	1.11

*Predefined values according to ref.[58]

Diamanti *et al.* found that the specific capacitance of a DOPC/DOPS lipid bilayer formed at PAH/PSS multilayer is in the range from 10 to 14 $\boldsymbol{\mu F cm^{-2}}$ and can be furthermore increased up to 36.5 $\boldsymbol{\mu F cm^{-2}}$ via sandwiching with subsequent polyelectrolyte layers.[23] Using eq. 1.4 we calculated the pseudocapacitance for a lipid bilayer as obtained from the best fit of an impedance spectrum from Figure 7. Although surprisingly high, 19.1 $\boldsymbol{\mu F cm^{-2}}$ is very similar to values reported by Diamanti. Corresponding thickness of a bilayer calculted using eq. 1.3 should be around 0.1 nm (assuming $\boldsymbol{\varepsilon}$ = 2) which make no physical sense. Such a low value can be rationalized as follows:

(i) As polyelectrolyte multilayers can induce a certain surface roughness[65],[66],[67] we can anticipate an increased surface area, which when increased by factor of 5 gives the value of specific capacitance equal to 3.8 $\boldsymbol{\mu F cm^{-2}}$;

(ii) Polyelectrolyte incorporation into the lipid bilayer framework[23],[68] can result in a higher dielectic constant[61] and consequently a higher electric capacitance.

(iii) Intact lipids vesicles can also reside within the lipid bilayer, which in consequence can also contribute to a number of defects;[69]

(iv) Lastly, the polyelectrolytes might affect the packing of lipids. The bilayer can be squeezed as the negatively charged polar head groups located at the outer leaflet can be electrostatically attracted by positive charge of underlining polyelectrolyte and/or we can imagine that lipids within the bilayer are simply tilted.

Considering an increased surface area and elevated dielectric constants (both a factor of 2 to 5 times) we would get a thickness of a lipid bilayer in a range of 0.4 to 2.3 nm, which is within the same order of magnitde as expected 4 – 5 nm thick bilayers. The low specific resistnace – 36.1 $\boldsymbol{k\Omega cm^2}$ – is a few orders of magnitude lower as compared with gigaseal properties of black lipid membranes. Fraction of defects can be estimated using:

$$\%_{defects} = A_{defects}/A_{Si} \tag{1.5}$$

where A_{Si} is the geometrical area of the silicon support ($7.9 \cdot 10^{-5}$ m^2) and $A_{defects}$ is given by:

$$A_{defects} = \frac{l_{LB}}{R_{LB}\kappa_{KCl}} \tag{1.6}$$

where l_{LB} is the thickness (5 nm) and R_{LB} the resistance of lipid bilayer (see above for the value) and κ_{KCl} is the conductivity of the background electrolyte within the membrane defect (around 0.1 Sm^{-1}). With all this information we get $A_{defects}$ = $1 \cdot 10^{-12}$ m^2 giving a fraction of defects equal to $2 \cdot 10^{-8}$. This proves that very small portion of defects within the lipid bilayer framework can lead to significant resistance drop.

3.5. Mobility of lipids at modified and unmodified SiO_2 surface

Fluorescent recovery after photobleaching was used to further confirm our findings based on EIS and OR. LVs composed from DOPC and the mixture of DOPC/DOPS (1:1 mole:mole) were doped with 0.5 wt.% of a Texas Red labeled 1,2-dioleoyl-*sn*-glycero-3-

phosphoethanolamine. As a support, we used glass wells that were activated with 1 M NaOH to ensure negative surface charge. We investigated the interaction between LVs (DOPC and DOPC/DOPS) and bare glass surface or glass surface modified with three polyelectrolyte layers in the following order: PEI, PSS and PAH.

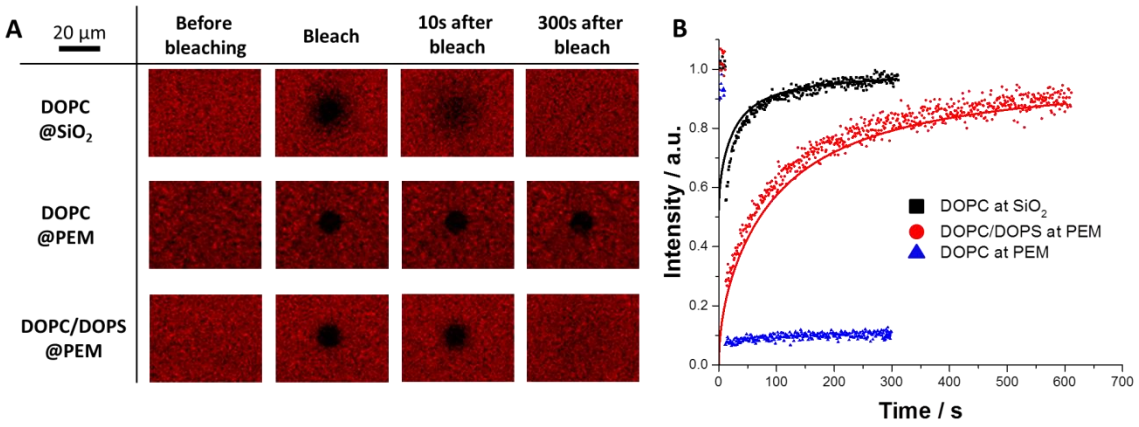

Figure 8. **(**A) Fluorescence emission from the supported lipid bilayer before, directly after, 10 s after and 300 s after bleaching. The surface composition is indicated in the left column. (B) Corresponding fluorescence recovery after bleaching plots (black squared – DOPC SLB at SiO_2; red circles – DOPC/DOPS SLB at polyelectrolyte layer and blue triangles – DOPC LVs at polyelectrolyte layer) together with the best fit (solid lines).

As expected, no fluorescence emission from the surface was detected after addition and subsequent incubation of DOPC/DOPS LVs over negatively charged glass surface layer (data not shown). Fluorescent emission from the surface was observed for three other systems indicating the adsorption of LVs as shown in Figure 8. Once again, DOPC LVs with slightly negatively surface charge (around –5 $\boldsymbol{mV}$) were found to bind to both negatively charged surface of glass and a positively charged terminal layer of PAH. As shown in Figure 8A and B we observed fast recovery – approaching to 100% after about 100 s as shown in Figure S8 – of fluorescence for the DOPC LVs adsorbed to negatively charged surface of a glass indicating fusion of LVs followed by lipid bilayer formation. The lateral diffusion coefficient obtained from the fitting is 0.29 $\mu m^2 s^{-1}$, which is in line with values reported elsewhere.[70] DOPC LVs also adsorbed to positively charged (PAH-terminated) layers. In this case, we did not observe any recovery of the fluorescent emission for the bleach spot up to 300 s. We concluded that DOPC LVs strongly adsorb to the surface in the form of intact vesicles. Fusion of DOPC/DOPS

LVs and formation of lipid bilayer over PAH layer was also confirmed as almost 100% recovery was obtained The lateral diffusion coefficient of 0.079 $\mu m^2 s^{-1}$ that was extracted from fitting is significantly lower[71] than the expected value for fluid lipid bilayer.[70] It is however within the range of 0.02 – 0.1 $\mu m^2 s^{-1}$ obtained for dioleoylphosphatidic acid (DOPA), dimyristoylphosphatidlcholine (DMPC) and DMPC/DOPA deposited over PAH terminated multilayer at ambient conditions.[21] Values in the range of 10^{-10} $cm^2 s^{-1}$ were reported for the lipids in the gel phase[72] which can be excluded here as the transition temperature of used lipids is significantly below ambient temperature at which all experiments were performed. Lower lateral diffusion coefficient values obtained in this work can originate from: (i) strong adsorption of lipids to the functionalities of polyelectrolyte layer[73] hence the mobility of lipids can consequentially be lower within the bottom leaflet as compared with the upper leaflet of the bilayer; (ii) affected morphology – lipids tilt, increased mutual penetration – that can affect local bilayer viscosity and in consequence diffusivity and (iii) surface roughness induced by polyelectrolyte cushion. **Concluding remarks**

In this work, we used straightforward layer-by-layer deposition of polyelectrolytes over silica-covered silicon semiconductors with the ultimate goal to form a lipid terminated biointerface. The properties of such system were investigated with optical reflectometry, electrochemical impedance spectroscopy and fluorescent recovery after photobleaching. The polyelectrolyte consisted of three or four layers: PEI, PSS and PAH or PEI, PSS, PAH and PSS, depending on the charge of the LVs used. Formation of the lipid bilayer onto the polyelectrolyte cushion is challenging. We have observed the adsorption of LVs followed by their rupture and formation of a lipid bilayer for DOPC LVs over bare negatively charged SiO_2 surface and DOPS/DOPC LVs over a surface terminated with positively charged PAH layer. DOPC LVs were found to adsorb and remain intact at a positively charged PAH layer, as well as the LVs holding highest absolute surface charge, *i.e.*, negatively charged DOPS and positively charged DOTAD added to platform terminated with oppositely charged layer of polyelectrolyte. The mutual effect of the deposited surface charge on the charge carriers within silicon semiconductor could be followed with impedance spectroscopy as (i) the bias potential applied to the p- and n-doped Si affected the thickness of a DOPC lipid bilayer formed onto SiO_2 as indicated by the observed capacitance values and (ii) the adsorption of the

polyelectrolytes and LVs/LB could be track by following the impedance of the space charge region hold under weak depletion.

To conclude, polyelectrolytes exhibit complex interactions with lipid bilayers, which are not fully understood. The fusion of LVs is very much dependent on the electrostatic interactions between the chemical functionalities located on lipids polar head groups and within the polyelectrolytes chain. Undoubtedly, the great advantage of the studied system is the easiness of the polymeric cushion formation. The organic synthesis toolbox to prepare and functionalize polyelectrolytes is quite large, allowing tuning of the density of ionisable/charged functional groups, which may further improve SLB formation. This is of great interest, since such an approach would open new avenues in versatile support functionalisation with no or very little effort required.

Acknowledgements

This work was supported by NanoNextNL, a micro and nanotechnology consortium of the Government of The Netherlands and 130 partners. This work has also received funding from the European Research Council (ERC) under the European Union's Horizon 2020 research and innovation programme (grant agreement No 682444, PI LCPMdS). PJ is grateful for the Netherlands Organization for Scientific Research (NWO) (NWO-VIDI 723.012.106) for financial support. We acknowledge Dr Jasper van Weerd (formerly University of Twente, now Lipocoat BV) and Mr Aldo Brinkman for the initial experiments. Mr Remco Fokkink (Wageningen University, The Netherlands) is acknowledged for growing the silica layer over silicon wafers used for optical reflectometry measurements.

References

[1] E.T. Castellana, P.S. Cremer, Solid supported lipid bilayers: From biophysical studies to sensor design, Surf. Sci. Rep. 61 (2006) 429–444. doi:10.1016/j.surfrep.2006.06.001.

[2] G. Koçer, P. Jonkheijm, Guiding hMSC Adhesion and Differentiation on Supported Lipid Bilayers, Adv. Healthc. Mater. 6 (2017) 1 – 11. doi:10.1002/adhm.201600862.

[3] J. van Weerd, M. Karperien, P. Jonkheijm, Supported Lipid Bilayers for the Generation of Dynamic Cell-Material Interfaces, Adv. Healthc. Mater. 4 (2015) 2743–2779. doi:10.1002/adhm.201500398.

[4] E. Kalb, S. Frey, L.K. Tamm, Formation of supported planar bilayers by fusion of vesicles to supported phospholipid monolayers, Biochim. Biophys. Acta. 1103 (1992) 307–316. doi:10.1016/0005-2736(92)90101-Q.

[5] P. Nollert, H. Kiefer, F. Jahnig, Lipid Vesicle Adsorption versus Formation of Planar Bilayers on Solid Surfaces, Biophys. J. 69 (1995) 1447–1455. doi:10.1016/S0006-3495(95)80014-7.

[6] C. Steinem, a Janshoff, W.P. Ulrich, M. Sieber, H.J. Galla, Impedance analysis of supported lipid bilayer membranes: a scrutiny of different preparation techniques., Biochim. Biophys. Acta. 1279 (1996) 169–180. doi:10.1016/0005-2736(95)00274-X.

[7] S.S. Mornet, O. Lambert, E. Duguet, A. Brisson, The formation of supported lipid bilayers on silica nanoparticles revealed by cryoelectron microscopy, Nano Lett. 5 (2005) 281–285. doi:10.1021/nl048153y.

[8] F. Wang, J. Liu, A stable lipid/TiO2 interface with headgruop-inversed phosphocholine and a comparison with SiO2, J. Am. Chem. Soc. 137 (2015) 11736–11742. doi:10.1021/jacs.5b06642.

[9] H. Schönherr, J.M. Johnson, P. Lenz, C.W. Frank, S.G. Boxer, Vesicle adsorption and lipid bilayer formation on glass studied by atomic force microscopy, Langmuir. 20 (2004) 11600–11606. doi:10.1021/la049302v.

[10] P.S. Cremer, S.G. Boxer, Formation and Spreading of Lipid Bilayers on Planar Glass Supports, J. Phys. Chem. B. 103 (1999) 2554–2559. doi:10.1021/jp983996x.

[11] R.P. Richter, R. Derat, A.R. Brisson, Formation of Supported Lipid Bilayers Formation of Solid-Supported Lipid Bilayers: An Integrated View, Langmuir. 22 (2006) 3497–3505.

[12] W. Knoll, C.W. Frank, C. Heibel, R. Naumann, A. Offenhäusser, J. Rühe, E.K. Schmidt, W.W. Shen, A. Sinner, Functional tethered lipid bilayers, Rev. Mol. Biotechnol. 74 (2000) 137–158. doi:10.1016/j.bbabio.2008.03.008.

[13] J. Lin, J. Szymanski, P. Chsearson, K. Hristova, Effect of a polymer cushion on the electrical properties and stability of surface-supported lipid bilayers, Langmuir. 26 (2010) 3544–3548. doi:10.1021/la903232b.

[14] V. Nikolov, J. Lin, M. Merzlyakov, K. Hristova, P.C. Searson, Electrical measurements of bilayer membranes formed by Langmuir-Blodgett deposition on single-crystal silicon, Langmuir. 23 (2007) 13040–13045. doi:10.1021/la702147m.

[15] C. a. Naumann, O. Prucker, T. Lehmann, J. Rühe, W. Knoll, C.W. Frank, The polymer-supported phospholipid bilayer: Tethering as a new approach to substrate-membrane stabilization, Biomacromolecules. 3 (2002) 27–35. doi:10.1021/bm0100211.

[16] S. Lingler, I. Rubinstein, W. Knoll, A. Offenhäusser, Fusion of Small Unilamellar Lipid Vesicles to Alkanethiol and Thiolipid Self-Assembled Monolayers on Gold, Langmuir. 13 (1997) 7085–7091. doi:10.1021/la970600k.

[17] K. Kumar, L. Isa, A. Egner, R. Schmidt, M. Textor, E. Reimhult, Formation of nanopore-spanning lipid bilayers through liposome fusion, Langmuir. 27 (2011) 10920–10928. doi:10.1021/la2019132.

[18] M. Tanaka, E. Sackmann, Polymer-supported membranes as models of the cell surface., Nature. 437 (2005) 656–663. doi:10.1038/nature04164.

[19] G. Decher, Fuzzy Nanoassemblies: Toward Layered Polymeric Multicomposites, Science (80-.). 277 (1997) 1232–1237. doi:10.1126/science.277.5330.1232.

[20] J.J. Richardson, J. Cui, M. Björnmalm, J.A. Braunger, H. Ejima, F. Caruso, Innovation in Layer-by-Layer Assembly, Chem. Rev. 116 (2016) 14828–14867. doi:10.1021/acs.chemrev.6b00627.

[21] T. Cassier, A. Sinner, A. Offenhäuser, H. Möhwald, Homogeneity, electrical resistivity and lateral diffusion of lipid bilayers coupled to polyelectrolyte multilayers, Colloids Surfaces B Biointerfaces. 15 (1999) 215–225. doi:10.1016/S0927-7765(99)00090-9.

[22] M. Fischlechner, M. Zaulig, S. Meyer, I. Estrela-Lopis, L. Cuéllar, J. Irigoyen, P. Pescador, M. Brumen, P. Messner, S. Moya, E. Donath, Lipid layers on polyelectrolyte multilayer supports, Soft Matter. 4 (2008) 2245–2258. doi:10.1039/b805754k.

[23] E. Diamanti, D. Gregurec, M.J. Rodríguez-Presa, C.A. Gervasi, O. Azzaroni, S.E. Moya, High resistivity lipid bilayers assembled on polyelectrolyte multilayer cushions: An impedance study, Langmuir. 32 (2016) 6263–6271. doi:10.1021/acs.langmuir.6b01191.

[24] E. Diamanti, P. Andreozzi, R. Anguiano, L. Yate, D. Gregurec, N. Politakos, R.F. Ziolo, E. Donath, S.E. Moya, The effect of top-layer chemistry on the formation of supported lipid bilayers on polyelectrolyte multilayers: primary versus quaternary amines, Phys. Chem. Chem. Phys. 18 (2016) 32396–32405. doi:10.1039/C6CP06258J.

[25] V. Atanasov, N. Knorr, R.S. Duran, S. Ingebrandt, A. Offenhäusser, W. Knoll, I. Köper, Membrane on a chip: a functional tethered lipid bilayer membrane on silicon oxide surfaces., Biophys. J. 89 (2005) 1780–1788. doi:10.1529/biophysj.105.061374.

[26] J. Lin, M. Merzlyakov, K. Hristova, P.C. Searson, Impedance spectroscopy of bilayer membranes on single crystal silicon., Biointerphases. 3 (2008) FA33–FA40. doi:10.1116/1.2896117.

[27] O. Purrucker, H. Hillebrandt, K. Adlkofer, M. Tanaka, Deposition of highly resistive lipid bilayer on silicon-silicon dioxide electrode and incorporation of gramicidin studied by ac impedance spectroscopy, Electrochim. Acta. 47 (2001) 791–798. doi:10.1016/S0013-4686(01)00759-9.

[28] C. Kataoka-Hamai, H. Inoue, Y. Miyahara, Detection of supported lipid bilayers using their electric charge., Langmuir. 24 (2008) 9916–20. doi:10.1021/la801623m.

[29] N. Misra, J.A. Martinez, S.-C.C.J. Huang, Y. Wang, P. Stroeve, C.P. Grigoropoulos, A. Noy, Bioelectronic silicon nanowire devices using functional membrane proteins.,

Proc. Natl. Acad. Sci. U. S. A. 106 (2009) 13780–13784. doi:10.1073/pnas.0904850106.

[30] M. Khan, N. Dosoky, D. Patel, J. Weimer, J. Williams, Lipid Bilayer Membrane in a Silicon Based Micron Sized Cavity Accessed by Atomic Force Microscopy and Electrochemical Impedance Spectroscopy, Biosensors. 7 (2017) 1–12. doi:10.3390/bios7030026.

[31] G.Z. Garyfallou, L.C.P.M. De Smet, E.J.R. Sudhölter, The effect of the type of doping on the electrical characteristics of electrolyte-oxide-silicon sensors: PH sensing and polyelectrolyte adsorption, Sensors Actuators, B Chem. 168 (2012) 207–213. doi:10.1016/j.snb.2012.04.010.

[32] Zeta Potential theory - chapter 16 - Malvern Instruments, n.d.

[33] J.C. Dijt, M.A.C. Stuart, G.J. Fleer, Reflectometry as a tool for adsorption studies, Adv. Colloid Interface Sci. 50 (1994) 79–101. doi:10.1016/0001-8686(94)80026-X.

[34] L. Lee, A.P.R. Johnson, F. Caruso, Manipulating the salt and thermal stability of DNA multilayer films via oligonucleotide length, Biomacromolecules. 9 (2008) 3070–3078. doi:10.1021/bm800593t.

[35] H. Pera, T.M. Nolte, F.A.M. Leermakers, J.M. Kleijn, Coverage and disruption of phospholipid membranes by oxide nanoparticles, Langmuir. 30 (2014) 14581–14590. doi:10.1021/la503413w.

[36] D.M. Soumpasis, Theoretical analysis of fluorescence photobleaching recovery experiments, Biophys. J. 41 (1983) 95–97. doi:10.1016/S0006-3495(83)84410-5.

[37] C. Chaiyasut, Y. Takatsu, S. Kitagawa, T. Tsuda, Estimation of the dissociation constants for functional groups on modified and unmodified silica gel supports from the relationship between electroosmotic flow velocity and pH, Electrophoresis. 22 (2001) 1267–1272. doi:10.1002/1522-2683(200105)22:7<1267::AID-ELPS1267>3.0.CO;2-8.

[38] C. Tabor, H. Tabor, Polyamines, 2011. http://medcontent.metapress.com/index/A65RM03P4874243N.pdf\nhttp://www.annualreviews.org/doi/pdf/10.1146/annurev.bi.53.070184.003533.

[39] S.E. Burke, C.J. Barrett, Swelling behavior of hyaluronic acid/polyallylamine hydrochloride multilayer films, Biomacromolecules. 6 (2005) 1419–1428. doi:10.1021/bm0492834.

[40] S.R. Lewis, S. Datta, M. Gui, E.L. Coker, F.E. Huggins, S. Daunert, L. Bachas, D. Bhattacharyya, Reactive nanostructured membranes for water purification, Proc. Natl. Acad. Sci. 108 (2011) 8577–8582. doi:10.1073/pnas.1101144108.

[41] K. Tang, N.A.M. Besseling, Formation of polyelectrolyte multilayers: ionic strengths and growth regimes, Soft Matter. 12 (2016) 1032–1040. doi:10.1039/C5SM02118A.

[42] Z. Cao, P.I. Gordiichuk, K. Loos, E.J.R. Sudhölter, L.C.P.M. de Smet, The effect of guanidinium functionalization on the structural properties and anion affinity of polyelectrolyte multilayers, Soft Matter. 12 (2016) 1496–1505. doi:10.1039/C5SM01655J.

[43] R. Mészáros, I. Varga, T. Gilányi, Adsorption of poly(ethyleneimine) on silica surfaces: Effect of pH on the reversibility of adsorption, Langmuir. 20 (2004) 5026–5029. doi:10.1021/la049611l.

[44] H. Hauser, The conformation of the polar group of lecithin and lysolecithin, J. Colloid Interface Sci. 55 (1976) 85–93. doi:10.1016/0021-9797(76)90012-6.

[45] E. Chibowski, A. Szczes, Zeta potential and surface charge of DPPC and DOPC liposomes in the presence of PLC enzyme, Adsorption. 22 (2016) 755–765. doi:10.1007/s10450-016-9767-z.

[46] H.I. Petrache, S. Tristram-Nagle, K. Gawrisch, D. Harries, V.A. Parsegian, J.F. Nagle, Structure and Fluctuations of Charged Phosphatidylserine Bilayers in the Absence of Salt, Biophys. J. 86 (2004) 1574–1586. doi:10.1016/S0006-3495(04)74225-3.

[47] C.A. Betty, R. Lal, J. V. Yakhmi, Impedance model of electrolyte-insulator-semiconductor structure with porous silicon semiconductor, Electrochim. Acta. 54 (2009) 3781–3787. doi:10.1016/j.electacta.2009.01.071.

[48] M. Chemla, V. Bertagna, R. Erre, F. Rouelle, S. Petitdidier, D. Levy, R and C Impedance Components Equivalent to the Charge Distribution within Si-Substrate Depletion Layer, Electrochem. Solid-State Lett. 6 (2003) G7–G11. doi:10.1149/1.1524752.

[49] V. Bertagna, R. Erre, F. Rouelle, M. Chemla, S. Petitdidier, D. Lévy, Electrochemical Study for the Characterization of Wet Silicon Oxide Surfaces, Solid State Phenom. 76-77 (2001) 81–84. doi:10.4028/www.scientific.net/SSP.76-77.81.

[50] M. Naumowicz, Z.A. Figaszewski, L. Poltorak, Electrochemical impedance spectroscopy as a useful method for examination of the acid–base equilibria at interface separating electrolyte solution and phosphatidylcholine bilayer, Electrochim. Acta. 91 (2013) 367–372. doi:10.1016/j.electacta.2012.12.093.

[51] A.D. Petelska, Z.A. Figaszewski, Interfacial tension of bilayer lipid membrane formed from phosphatidylethanolamine, Biochim. Biophys. Acta - Biomembr. 1567 (2002) 79–86. doi:10.1016/S0005-2736(02)00582-5.

[52] M. Naumowicz, A.D. Petelska, Z.A. Figaszewski, Impedance analysis of phosphatidylcholine-cholesterol system in bilayer lipid membranes, Electrochim. Acta. 50 (2005) 2155–2161. doi:10.1016/j.electacta.2004.09.023.

[53] M. Naumowicz, A.D. Petelska, Z.A. Figaszewski, Impedance analysis of a phosphatidylcholine-phosphatidylethanolamine system in bilayer lipid membranes, Electrochim. Acta. 51 (2006) 5024–5028. doi:10.1016/j.electacta.2006.03.038.

[54] M. Naumowicz, Z.A. Figaszewski, The Effect of pH on the Electrical Capacitance of Phosphatidylcholine-Phosphatidylserine System in Bilayer Lipid Membrane., J. Membr. Biol. 247 (2014) 361–9. doi:10.1007/s00232-014-9644-1.

[55] S.H. White, Formation of "solvent-free" black lipid bilayer membranes from glyceryl monooleate dispersed in squalene., Biophys. J. 23 (1978) 337–347. doi:10.1016/S0006-3495(78)85453-8.

[56] J.P. Dilger, S.G. McLaughlin, T.J. McIntosh, S.A. Simon, The dielectric constant of phospholipid bilayers and the permeability of membranes to ions., Science. 206 (1979) 1196–1198. doi:10.1126/science.228394.

[57] M.J. Higgins, M. Polcik, T. Fukuma, J.E. Sader, Y. Nakayama, S.P. Jarvis, Structured water layers adjacent to biological membranes., Biophys. J. 91 (2006) 2532–2542. doi:10.1529/biophysj.106.085688.

[58] T.H. Silva, V. Garcia-Morales, C. Moura, J.A. Manzanares, F. Silva, Electrochemical impedance spectroscopy of polyelectrolyte multilayer modified gold electrodes: Influence of supporting electrolyte and temperature, Langmuir. 21 (2005) 7461–7467. doi:10.1021/la0507176.

[59] J. Zhao, C.R. Bradbury, D.J. Fermín, Long-range electronic communication between metal nanoparticles and electrode surfaces separated by polyelectrolyte multilayer films, J. Phys. Chem. C. 112 (2008) 6832–6841. doi:10.1021/jp710167y.

[60] S.V.P. Barreira, V. García-Morales, C.M. Pereira, J.A. Manzanares, F. Silva, Electrochemical Impedance Spectroscopy of Polyelectrolyte Multilayer Modified Electrodes, J. Phys. Chem. B. 108 (2004) 17973–17982. doi:10.1021/jp0466845.

[61] P.A. Neff, B.K. Wunderlich, R. V. Klitzing, A.R. Bausch, Formation and dielectric properties of polyelectrolyte multilayers studied by a silicon-on-insulator based thin film resistor, Langmuir. 23 (2007) 4048–4052. doi:10.1021/la063632t.

[62] J. Fritz, E.B. Cooper, S. Gaudet, P.K. Sorger, S.R. Manalis, Electronic detection of DNA by its intrinsic molecular charge, Proc. Natl. Acad. Sci. 99 (2002) 14142–14146. doi:10.1073/pnas.232276699.

[63] F. Uslu, S. Ingebrandt, D. Mayer, S. Böcker-Meffert, M. Odenthal, A. Offenhäusser, Labelfree fully electronic nucleic acid detection system based on a field-effect transistor device, Biosens. Bioelectron. 19 (2004) 1723–1731. doi:10.1016/j.bios.2004.01.019.

[64] R. Klitzing, H. Moehwald, Proton Concentration Profile in Ultrathin Polyelectrolyte Films, Langmuir. 11 (1995) 3554–3559. doi:10.1021/la00009a044.

[65] R.A. McAloney, M. Sinyor, V. Dudnik, M. Cynthia Goh, Atomic force microscopy studies of salt effects on polyelectrolyte multilayer film morphology, Langmuir. 17 (2001) 6655–6663. doi:10.1021/la010136q.

[66] O. Mermut, J. Lefebvre, D.G. Gray, C.J. Barrett, Structural and mechanical properties of polyelectrolyte multilayer films studied by AFM, Macromolecules. 36 (2003) 8819–8824. doi:10.1021/ma034967+.

[67] P. Lavalle, C. Gergely, F.J.G. Cuisinier, G. Decher, P. Schaaf, J.C. Voegel, C. Picart, Comparison of the Structure of Polyelectrolyte Multilayer Films Exhibiting a Linear and an Exponential Growth Regime: An in Situ Atomic Force Microscopy Study, Macromolecules. 35 (2002) 4458–4465. doi:10.1021/ma0119833.

[68] N. Wilkosz, D. Jamróz, W. Kopec, K. Nakai, S. Yusa, M. Wytrwal-Sarna, J. Bednar, M. Nowakowska, M. Kepczynski, Effect of Polycation Structure on Interaction with Lipid Membranes, J. Phys. Chem. B. (2017) acs.jpcb.7b05248. doi:10.1021/acs.jpcb.7b05248.

[69] R.P. Richter, R.R. Escarpit, P. Cedex, Formation of Solid-Supported Lipid Bilayers: An Integrated View Ralf, Langmuir. 22 (2006) 3497–3505.

[70] F. Pincet, V. Adrien, R. Yang, J. Delacotte, J.E. Rothman, W. Urbach, D. Tareste, FRAP to characterize molecular diffusion and interaction in various membrane environments, PLoS One. 11 (2016) 1–19. doi:10.1371/journal.pone.0158457.

[71] R. Macháň, M. Hof, Lipid diffusion in planar membranes investigated by fluorescence correlation spectroscopy, Biochim. Biophys. Acta - Biomembr. 1798 (2010) 1377–1391. doi:10.1016/j.bbamem.2010.02.014.

[72] L. Wang, M. Schonhoff, H. Mohwald, Swelling of Polyelectrolyte Multilayer-Supported Lipid Layers. 1. Layer Stability and Lateral Diffusion, J. Phys. Chem. B. 108 (2004) 4767–4774. doi:10.1021/jp036413e.

[73] E. Diamanti, L. Cuellar, D. Gregurec, S.E. Moya, E. Donath, Role of Hydrogen Bonding and Polyanion Composition in the Formation of Lipid Bilayers on Top of Polyelectrolyte Multilayers, Langmuir. 31 (2015) 8623–8632. doi:10.1021/acs.langmuir.5b01731.

Graphical Abstract